Electronic Supplementary Material (ESI) for Dalton Transactions.
This journal is © The Royal Society of Chemistry 2018

Supporting Information

A two-fold 2D + 2D → 2D interweaved rhombus (4,4) grid: synthesis, structure, and dye removal properties in darkness and in daylight

Meng-Jung Tsai, Jheng-Hua Luo, and Jing-Yun Wu*

Department of Applied Chemistry, National Chi Nan University, Nantou 545, Taiwan. E-mail: jyunwu@ncnu.edu.tw

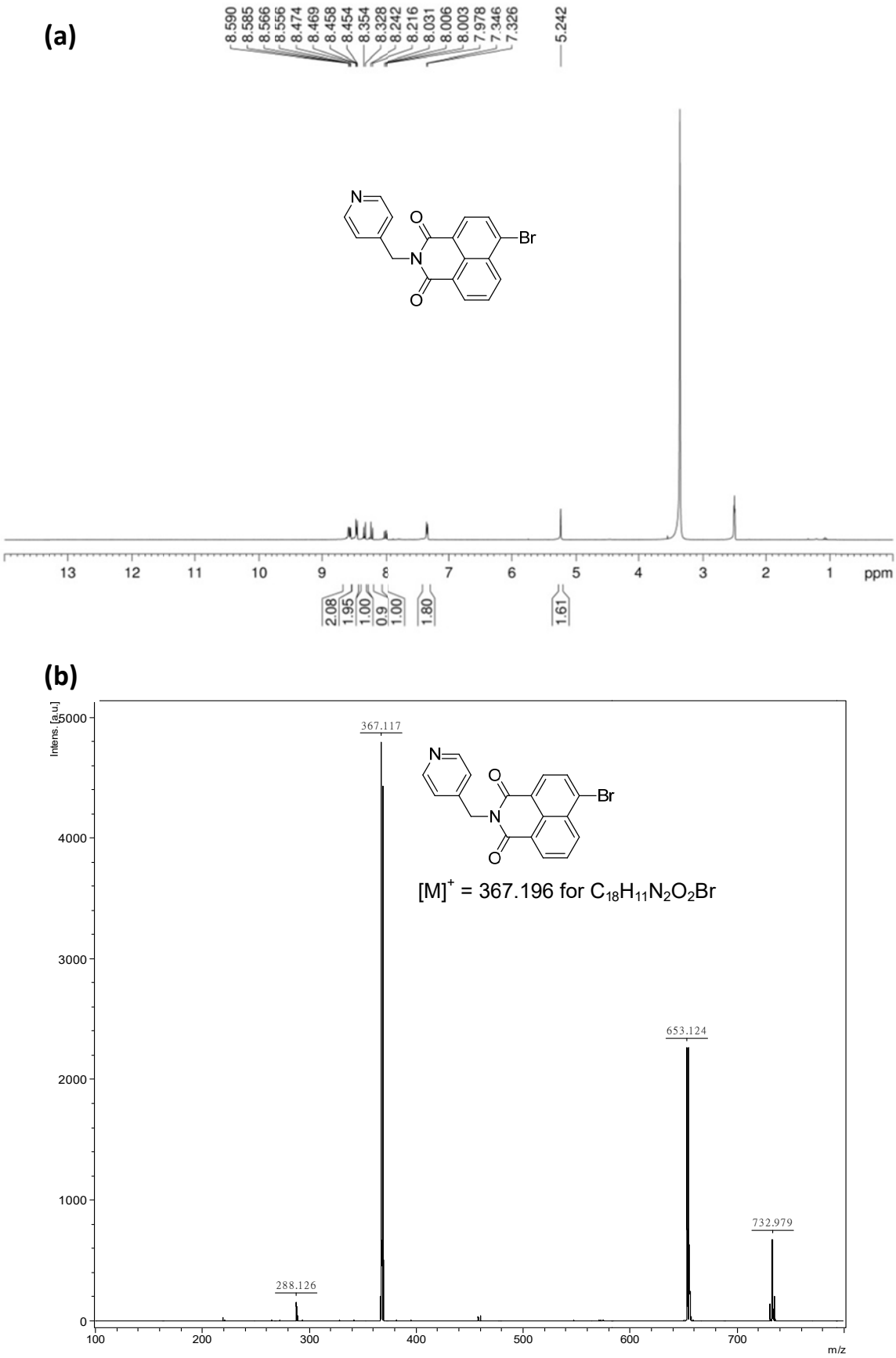

Fig. S1 (a) ^{1}H NMR (DMSO-d_6) and (b) MALDI-TOF MS spectra of *N*-(pyridin-4-ylmethyl)-4-bromo-1,8-naphthalimide

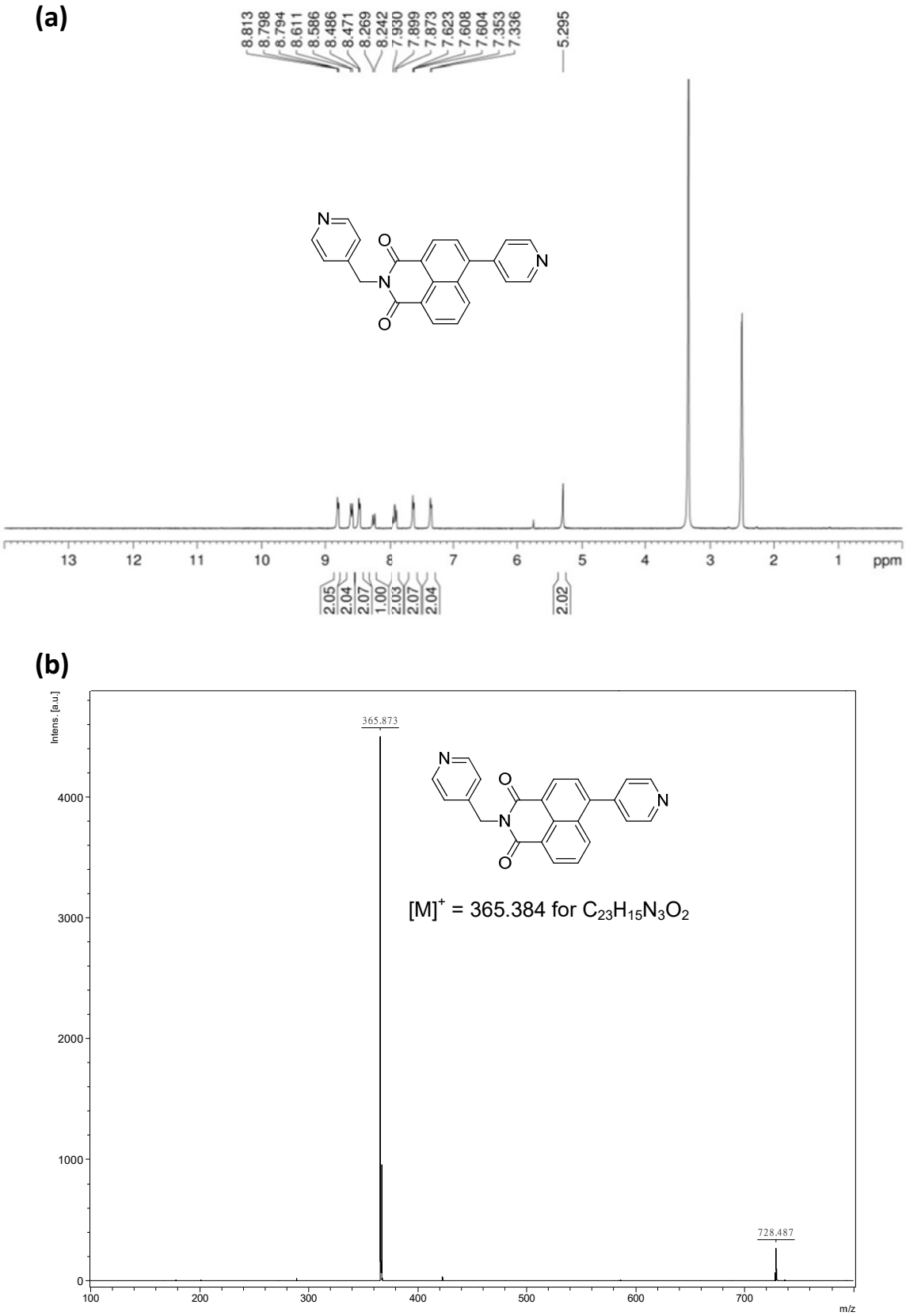

Fig. S2 (a) ^{1}H NMR (DMSO-d_6) and (b) MALDI-TOF MS spectra of NI-mbpy-44.

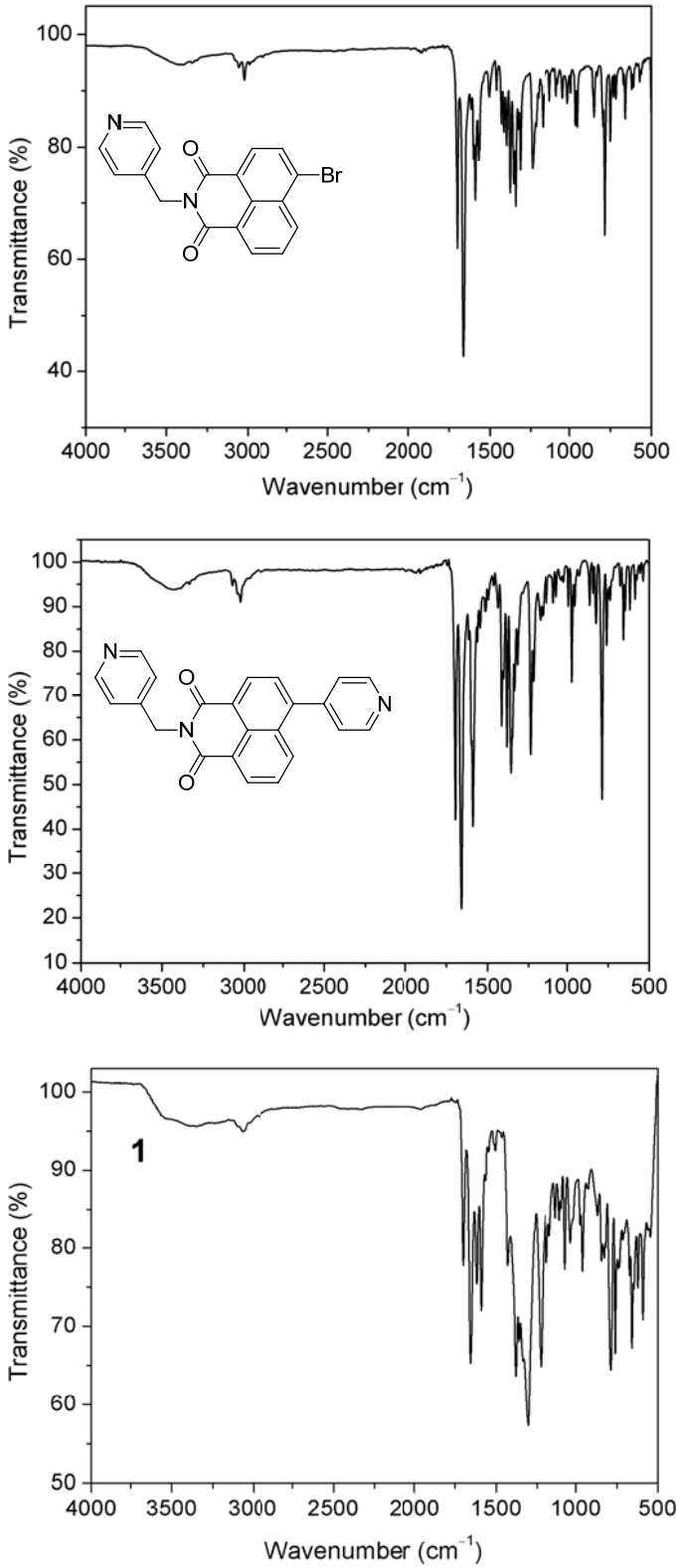

Fig. S3 IR spectra of *N*-(pyridin-4-ylmethyl)-4-bromo-1,8-naphthalimide, NI-mbpy-44, and **1**.

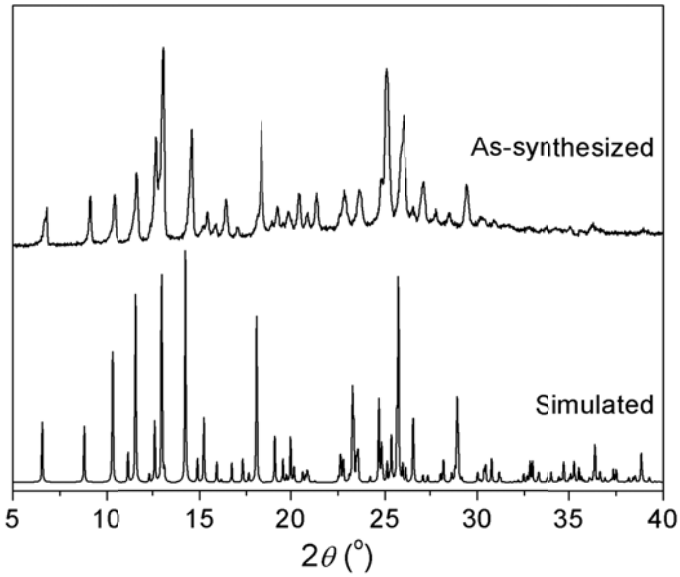

Fig. S4 XRPD patterns of simulated and as-synthesized **1**.

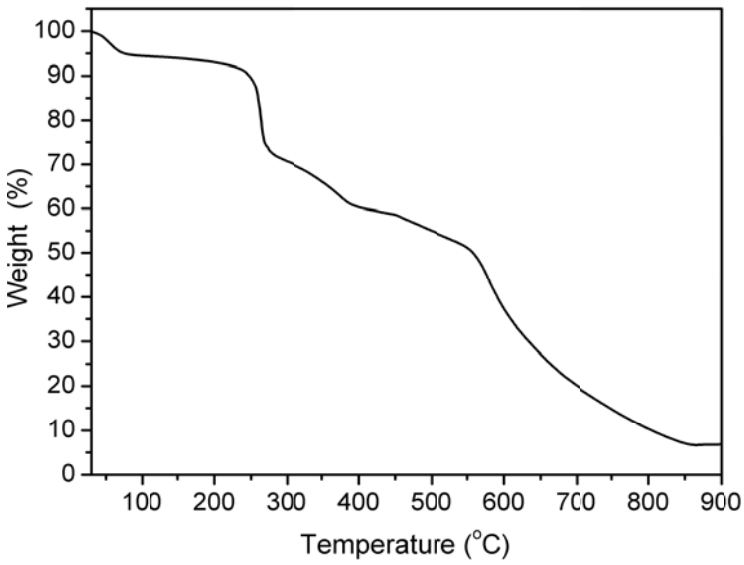

Fig. S5 TG curve of **1**

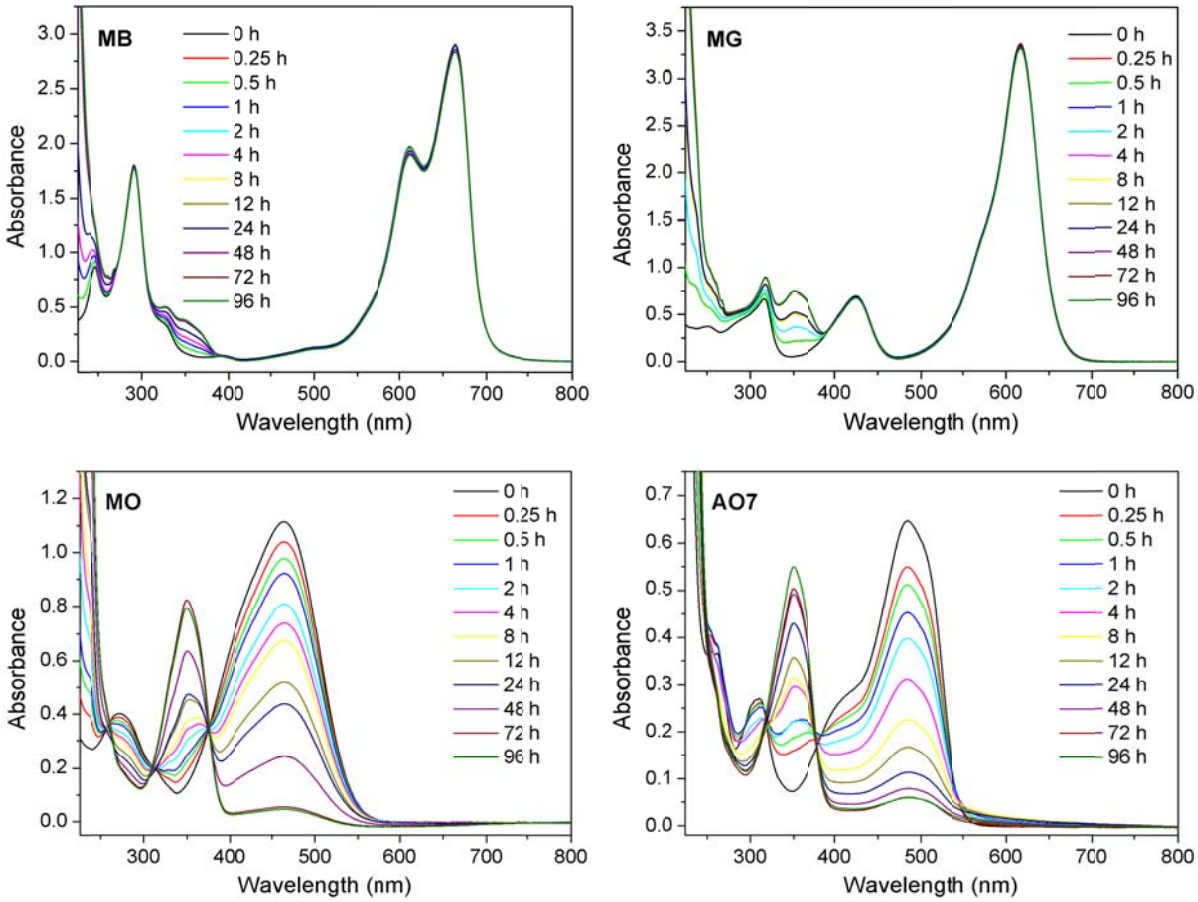

Fig. S6 UV-Vis spectra of aqueous solutions of MB, MG, MO, and AO7 (20 ppm) during a dye removal test with **1** over 0.25, 0.5, 1, 2, 4, 8, 12, 24, 48, 72, and 96 h in darkness at room temperature.

Fig. S7 Photographs of crystalline materials of **1** before and after immersion of MO and AO7.

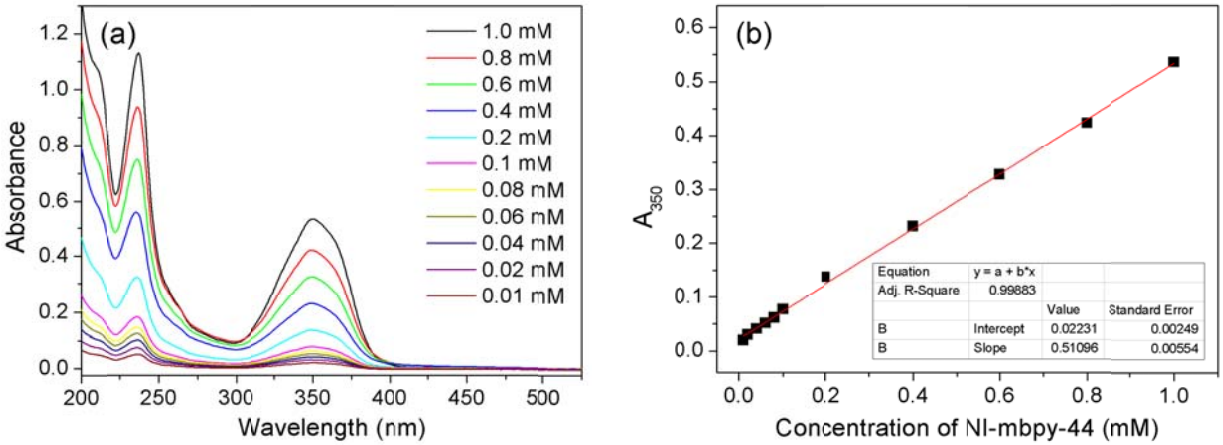

Fig. S8 (a) UV-Vis spectra of NI-mbpy-44 in water with various concentrations. (b) Calibration curve of NI-mbpy-44 in water.

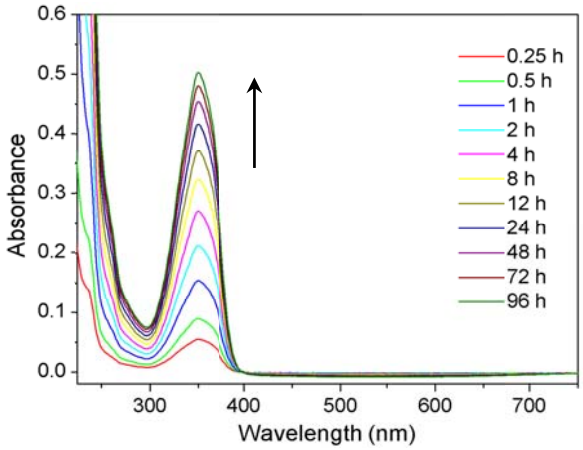

Fig. S9 UV-Vis spectra of **1** in water over 0.25, 0.5, 1, 2, 4, 8, 12, 24, 48, 72, and 96 h.

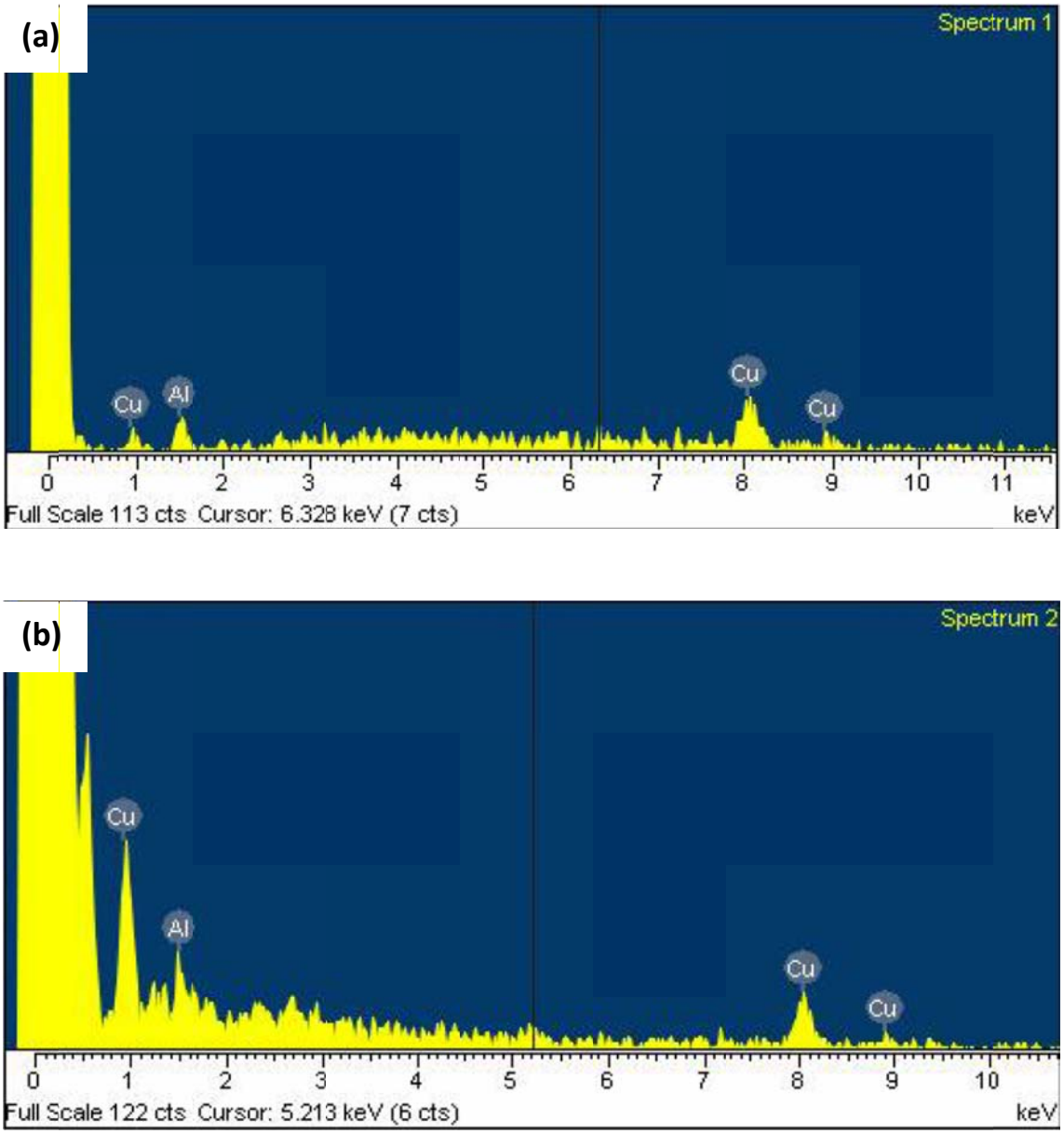

Fig. S10 EDX spectra of supernatants after removal of (a) MO and (b) AO7 by **1** for 96 h in darkness at room temperature.

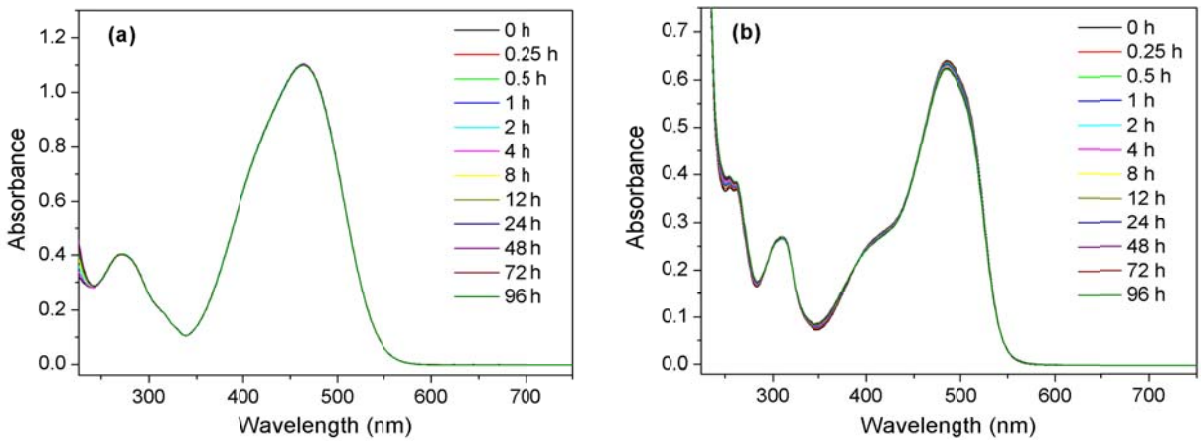

Fig. S11 UV-Vis spectra of (a) MO and (b) AO7 in the presence of $Cu(NO_3)_2{\cdot}2.5H_2O$ (0.01 mmol) in water (3 mL) with an initial dye concentration of 20 ppm at room temperature in darkness.

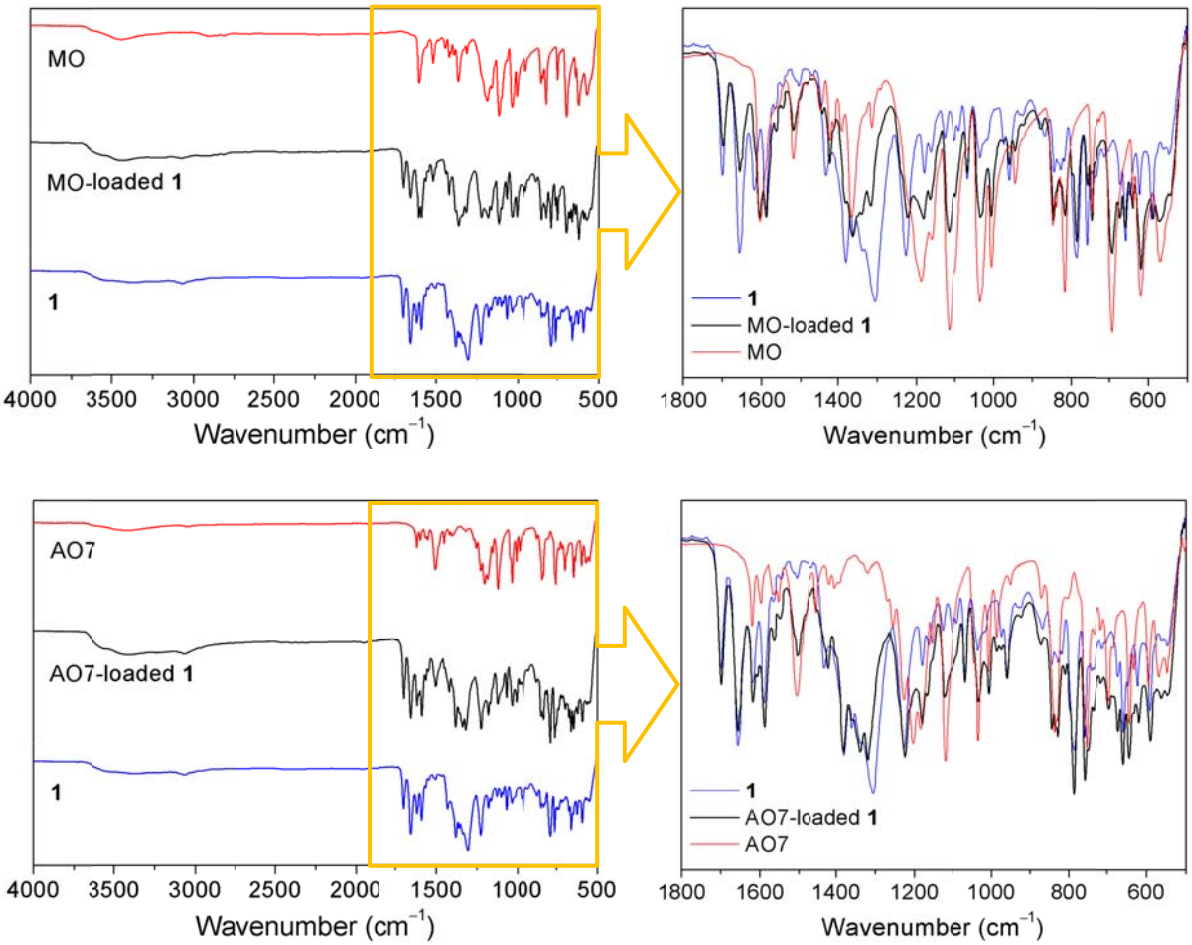

Fig. S12 Full (left) and expanded region (right) in IR spectra of **1**, dye, and dye-loaded **1** after removal of dye by **1** for 96 h.

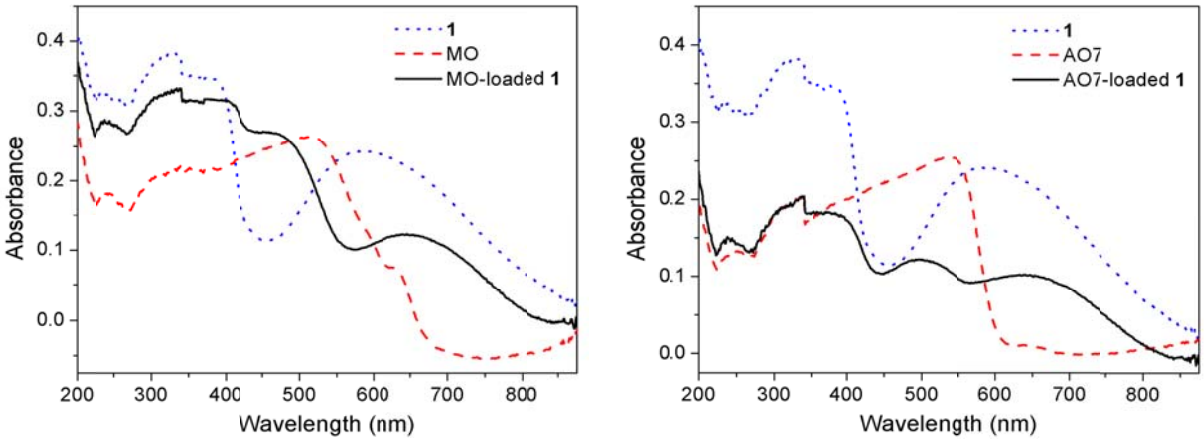

Fig. S13 Solid-state UV-Vis spectra of **1**, dye, and dye-loaded **1**.

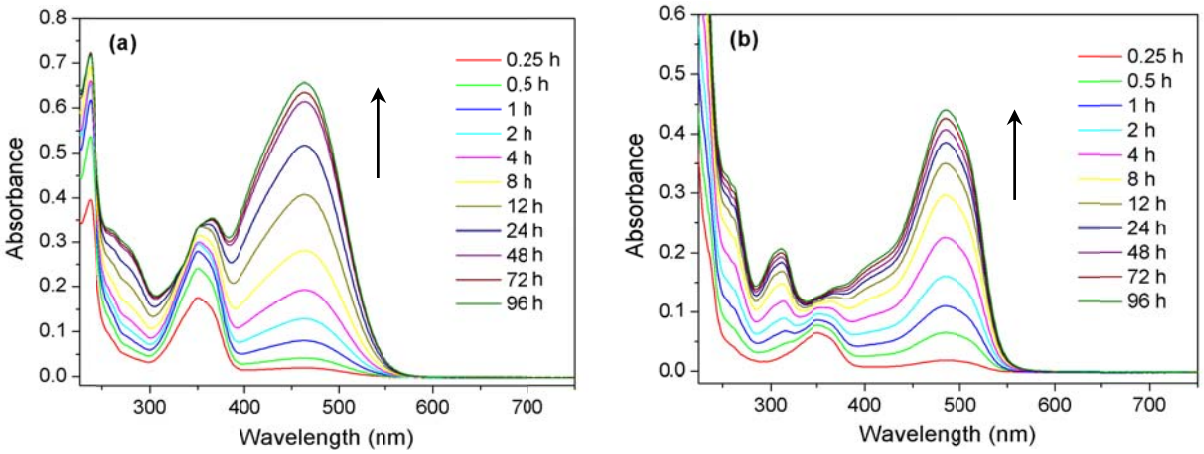

Fig. S14 UV-Vis spectra of (a) MO-loaded **1** and (b) AO7-loaded **1** in water, showing desorption of dye which has been adsorbed on the solid of **1**.

Particulate Systems

NanoPlus
Common

EOS Plot / Distribution Graph S/N : 400812

User	: Common	Group	:	Repetition	: 1/1
Date	: 2018/9/4	File Name	: 20180904-chu336-1		
Time	: 12:36:12	Sample Information	:		
SOP Name	: SOP(New)			Security	: No Security

Version 5.01 / 3.00

EOS Plot

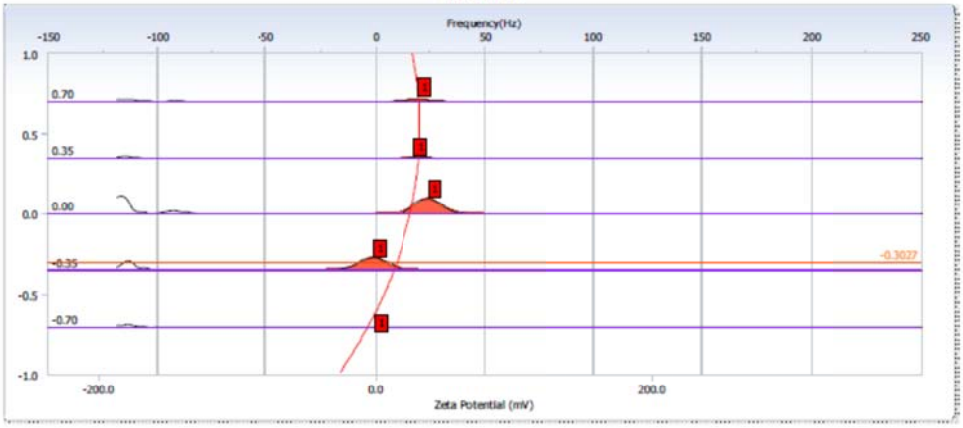

Mobility Distribution

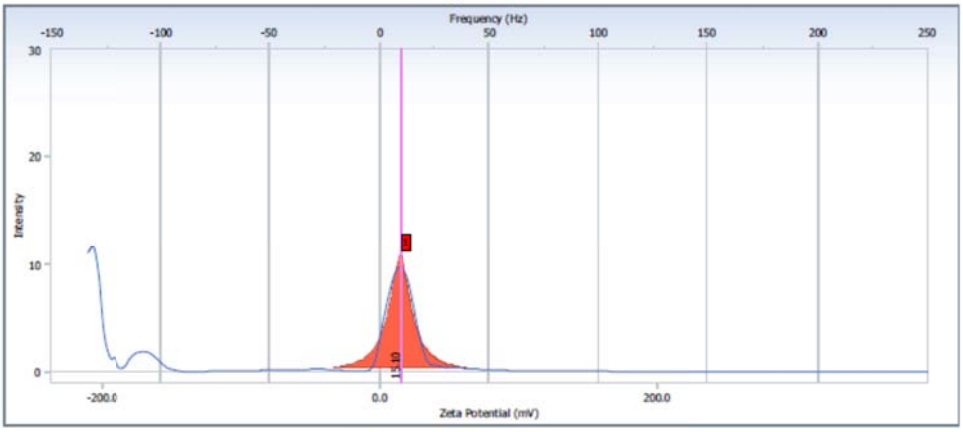

Measurement Results

Zeta Potential	: 15.10	(mV)	Doppler shift	: 9.57	(Hz)
Mobility	: 1.202e-004	(cm²/Vs)	Base Frequency	: 118.1	(Hz)
Conductivity	: 0.0197	(mS/cm)	Conversion Equation	: Smoluchowski	

Zeta Potential of Cell			Diluent Properties		
Upper Surface	: -12.55	(mV)	Diluent Name	: water-1	
Lower Surface	: 42.18	(mV)	Temperature	: 25.0	(°C)
Cell Condition			Refractive Index	: 1.3330	
Cell Type	: Flow Cell		Viscosity	: 0.8904	(cP)
Avg. Electric Field	: 16.61	(V/cm)	Dielectric Constant	: 80.2	
Avg. Current	: 0.02	(mA)			

Fig. S15 Zeta potential measurement of **1** in water.

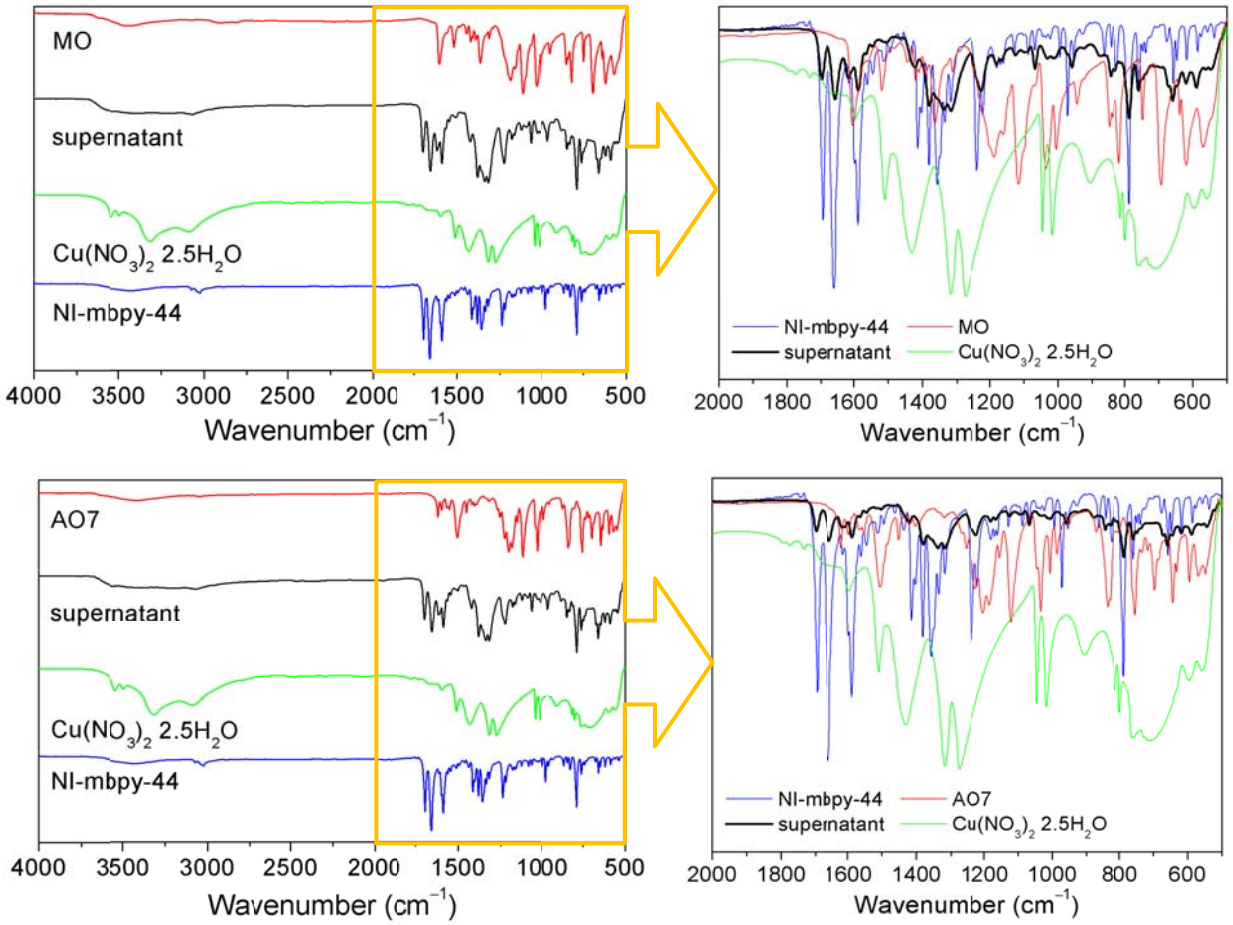

Fig. S16 Full (left) and expanded region (right) in IR spectra of supernatant after removal of dye by **1** for 96 h and free NI-mbpy-44, dye, and $Cu(NO_3)_2{\cdot}2.5H_2O$.

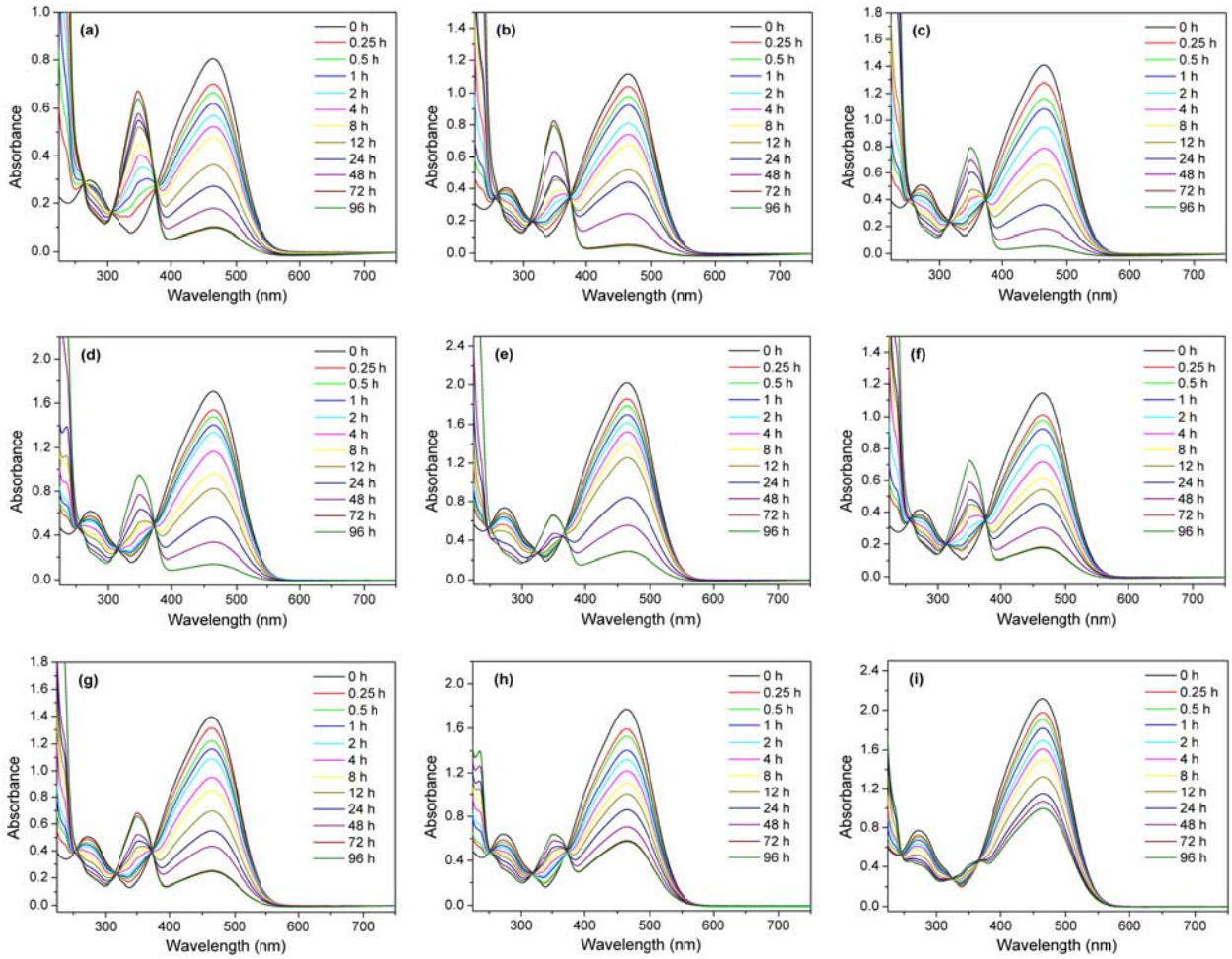

Fig. S17 UV-Vis spectra of aqueous solutions of MO during an adsorption with **1** at initial dye concentrations of (a) 10 ppm, (b) 20 ppm, (c) 30 ppm, (d) 40 ppm, (e) 50 ppm, (f) 100 ppm, (g) 150 ppm, (h) 200 ppm, and (i) 250 ppm over 0.25, 0.5, 1, 2, 4, 8, 12, 24, 48, 72, and 96 h in darkness at room temperature.

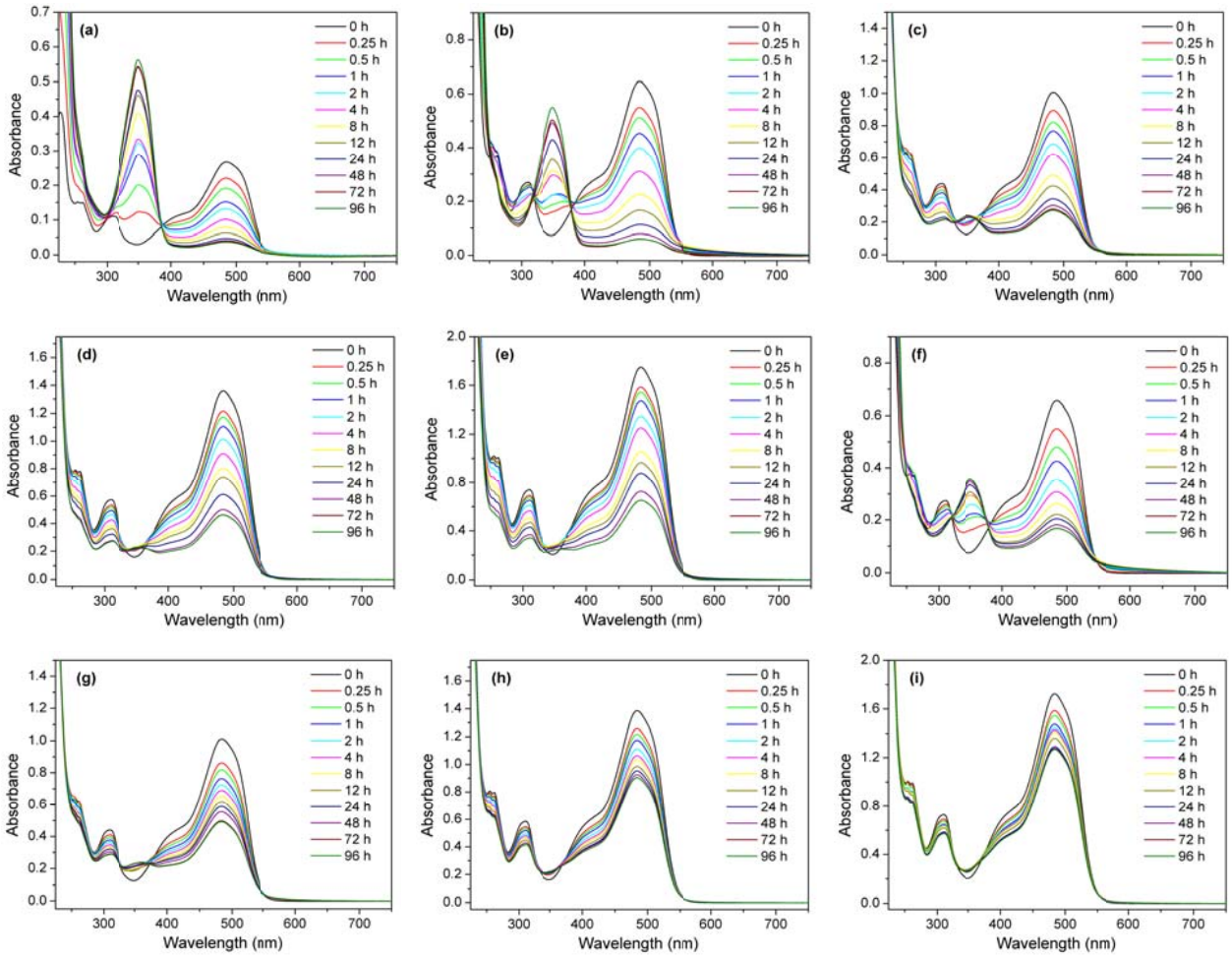

Fig. S18 UV-Vis spectra of aqueous solutions of AO7 during an adsorption with **1** at initial dye concentrations of (a) 10 ppm, (b) 20 ppm, (c) 30 ppm, (d) 40 ppm, (e) 50 ppm, (f) 100 ppm, (g) 150 ppm, (h) 200 ppm, and (i) 250 ppm over 0.25, 0.5, 1, 2, 4, 8, 12, 24, 48, 72, and 96 h in darkness at room temperature.

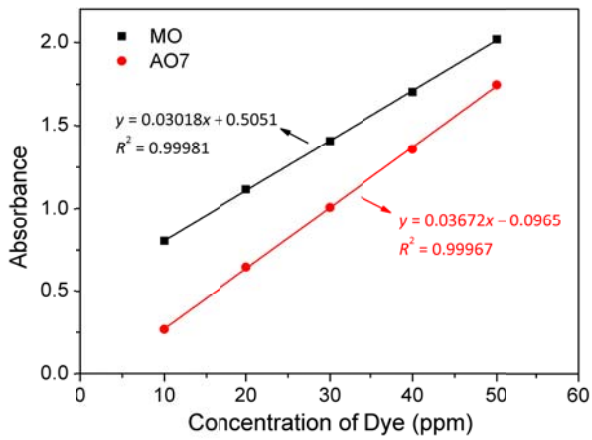

Fig. S19 Calibration curves of MO and AO7 in water in darkness at room temperature.

Table S1 Adsorption of MO and AO7 from water over various adsorbents

Dyes	Adsorbents	Amount adsorbed (mg g^{-1})	Ref.
MO	PCN-222	589	S1
	TMU-16-NH_2	393.7	S2
	1Y	1337	S3
	MIL-101(Cr)	114	S4
	ED-MIL-101(Cr)[a]	160	S4
	PED-MIL-101(Cr)[b]	194	S4
	NH_2-MIL-101(Al)	188	S5
	TiO_2@MIL-101	19.23	S6
	Fe_3O_4@MIL-101($Al_{0.9}Fe_{0.1}$)/NH_2	355.8	S7
	MIL-100(Fe)	1045	S8
	MIL-100(Cr)	211.8	S8
	UiO-66	39	S9
	UiO-66-NH_2	29	S9
	Ce(III)-doped UiO-66	639.6	S10
	Fe_3O_4@SiO_2@UiO-66 (MFC-O)	219	S11
	Fe_3O_4@SiO_2@UiO-66-NH_2 (MFC-N)	130	S11
	Fe_3O_4@SiO_2@UiO-66-Urea (MFC-U)	183	S11
	1 (in darkness)	810	This work
	1 (in daylight)	780	This work
	$[Cu(bipy)Cl_2]_n$	1084	S12
	$[Cu(bipy)SO_4]_n$	1521	S12
	MOF-235	477	S13
	ZIF-67	1340	S14
	Fe_3O_4@CTF[c]	291	S15
	Activated carbon (AC)	384	S16
	Fe_2O_3/AC composite	324	S16
AO7	UiO-66	332	S17
	1 (in darkness)	370	This work
	1 (in daylight)	360	This work
	Fe-BTC MOF	435	S18
	$[Cu(bipy)Cl_2]_n$	848	S12
	$[Cu(bipy)SO_4]_n$	3308	S12
	Al-SA	533	S19
	Sludge adsorbent	350	S20
	Activated carbon	404	S21
	Magnetic biochar/Fe_3O_4 nanocomposites	297	S22

[a]Ethylenediamine-grafted-MIL-101(Cr). [b]Protonated ethylenediamine-grafted-MIL-101(Cr).
[c]Covalent triazine-based framework/Fe_2O_3 composite.

References

(S1) H. Li, X. Cao, C. Zhang, Q. Yu, Z. Zhao, X. Niu, X. Sun, Y. Liu, L. Ma and Z. Li, *RSC Adv.*, 2017, **7**, 16273–16281.

(S2) M. Roushani, Z. Saedi and T. M. beygi, *J. Taiwan Inst. Chem. Eng.*, 2016, **66**, 164–171.

(S3) C.-Y. Gao, Y. Yang, J. Ai, H.-R. Tian, L.-J. Li, W. Yang, S. Dang and Z.-M. Sun, *Chem. Eur. J.*, 2016, **22**, 11652–11659.

(S4) E. Haque, J. Eun Lee, I. T. Jang, Y. K. Hwang, J.-S. Chang, J. Jegal and S. H. Jhung, *J. Hazard. Mater.*, 2010, **181**, 535–542.

(S5) E. Haque, V. Lo, A. I. Minett, A. T. Harris and T. L. Church, *J. Mater. Chem. A*, 2014, **2**, 193–203.

(S6) N. Chang, H. Zhang, M.-S. Shi, J. Li, W. Shao and H.-T. Wang, *Mater. Lett.*, 2017, **200**, 55–58.

(S7) S. Bao, K. Li, P. Ning, J. Peng, X. Jin and L. Tang, *J. Taiwan Inst. Chem. Eng.*, 2018, **87**, 64–72.

(S8) M. Tong, D. Liu, Q. Yang, S. Devautour-Vinot, G. Mauri and C. Zhong, *J. Mater. Chem. A*, 2013, **1**, 8534–8537.

(S9) Q. Chen, Q. He, M. Lv, Y. Xu, H. Yang, X. Liu and F. Wei, *Appl. Surf. Sci.*, 2015, **327**, 77–85.

(S10) J.-M. Yang, R.-J. Ying, C.-X. Han, Q.-T. Hu, H.-M. Xu, J.-H. Li, Q. Wang and W. Zhang, *Dalton Trans.*, 2018, **47**, 3913–3920.

(S11) L. Huang, M. He, B. Chen and B. Hu, *Chemosphere*, 2018, **199**, 435–444.

(S12) L. Xiao, Y. Xiong, Z. Wen and S. Tian, *RSC Adv.*, 2015, **5**, 61593–61600.

(S13) E. Haque, J. W. Jun and S. H. Jhung, *J. Hazard. Mater.*, 2011, **185**, 507–511.

(S14) Z.-h. Zhang, J.-l. Zhang, J.-m. Liu, Z.-h. Xiong and X. Chen, *Water Air Soil Pollut.*, 2016, **227**, 471.

(S15) W. Zhang, F. Liang, C. Li, L.-G. Qiu, Y.-P. Yuan, F.-M. Peng, X. Jiang, A.-J. Xie, Y.-H. Shen and J.-F. Zhu, *J. Hazard. Mater.*, 2011, **186**, 984–990.

(S16) R.-S. Juang, Y.-C. Yei, C.-S. Liao, K.-S. Lin, H.-C. Lu, S.-F. Wang and A.-C. Sun, *J. Taiwan Inst. Chem. Eng.*, 2018, **90**, 51–60.

(S17) K.-D. Zhang, F.-Ch. Tsai, N. Ma, Y. Xia, H.-L. Liu, X.-Q. Zhan, X.-Y. Yu, X.-Z. Zeng, T. Jiang, D. Shi and C.-J. Chang, *Materials*, 2017, **10**, 205.

(S18) E. R. García, R. L. Medina, M. M. Lozano, I. He. Pérez, M. J. Valero and A. M. M. Franco, *Materials*, 2014, **7**, 8037–8057.

(S19) K.-W. Jung, B. H. Choi, C. M. Dao, Y. J. Lee, J.-W. Choi, K.-H. Ahn and S.-H. Lee, *J. Ind. Eng. Chem.*, 2018, **59**, 149–159.

(S20) H.-M. Chiang, T.-C. Chen, S.-D. Pan and H.-L. Chiang, *J. Hazard. Mater.*, 2009, **161**, 1384–1390.

(S21) G. Zhang, J. Qu, H. Liu, A. T. Cooper and R. Wu, *Chemosphere*, 2007, **68**, 1058–1066.

(S22) K.-W. Jung, B. H. Choi, T.-U. Jeong and K.-H. Ahn, *Bioresour. Thechnol.*, 2016, **220**, 672–676.

Table S2 Pseudo-first-order and pseudo-second-order kinetic constants for the adsorption of MO and AO7 over **1** in darkness at room temperature[a]

				Pseudo-first-order kinetic model			Pseudo-second-order kinetic model		
Dye	Condition	C_i (ppm)	$Q_{e,exp}$ (mg g^{-1})	$Q_{e,calcd}$ (mg g^{-1})	k_1 (h^{-1})	R^2	$Q_{e,calcd}$ (mg g^{-1})	k_2 (g mg^{-1} h^{-1})	R^2
MO	Darkness	10	50	40	4.01×10^{-2}	0.9518	52	3.60×10^{-3}	0.9862
		20	113	96	2.95×10^{-2}	0.9425	118	9.99×10^{-4}	0.9627
		30	168	135	4.26×10^{-2}	0.9564	174	1.08×10^{-3}	0.9895
		40	222	191	3.59×10^{-2}	0.9707	234	5.54×10^{-4}	0.9769
		50	236	208	3.25×10^{-2}	0.9806	251	4.31×10^{-4}	0.9572
		100	518	410	3.53×10^{-2}	0.9278	532	3.35×10^{-4}	0.9833
		150	686	559	3.37×10^{-2}	0.9065	714	2.13×10^{-4}	0.9816
		200	785	596	4.01×10^{-2}	0.9339	806	2.75×10^{-4}	0.9898
		250	730	560	5.71×10^{-2}	0.9480	757	3.51×10^{-4}	0.9957
AO7	Darkness	10	49	27	7.31×10^{-2}	0.8797	49	1.36×10^{-2}	0.9995
		20	102	71	6.17×10^{-2}	0.9197	104	3.60×10^{-3}	0.9984
		30	112	75	6.40×10^{-2}	0.9087	114	3.63×10^{-3}	0.9987
		40	133	99	6.04×10^{-2}	0.9687	137	2.25×10^{-3}	0.9966
		50	157	115	5.26×10^{-2}	0.9325	161	1.78×10^{-3}	0.9960
		100	407	216	6.77×10^{-2}	0.8431	411	1.75×10^{-3}	0.9995
		150	395	220	3.65×10^{-2}	0.7468	395	1.09×10^{-3}	0.9946
		200	354	199	6.00×10^{-2}	0.8685	358	1.66×10^{-3}	0.9989
		250	329	187	7.87×10^{-2}	0.9233	334	1.96×10^{-3}	0.9988

[a] C_i, initial dye concentration; $Q_{e,exp}$, experimental adsorption capacity; $Q_{e,calcd}$, calculated adsorption capacity; k_1, pseudo-first-order kinetic constant; k_2, pseudo-second-order kinetic constant.

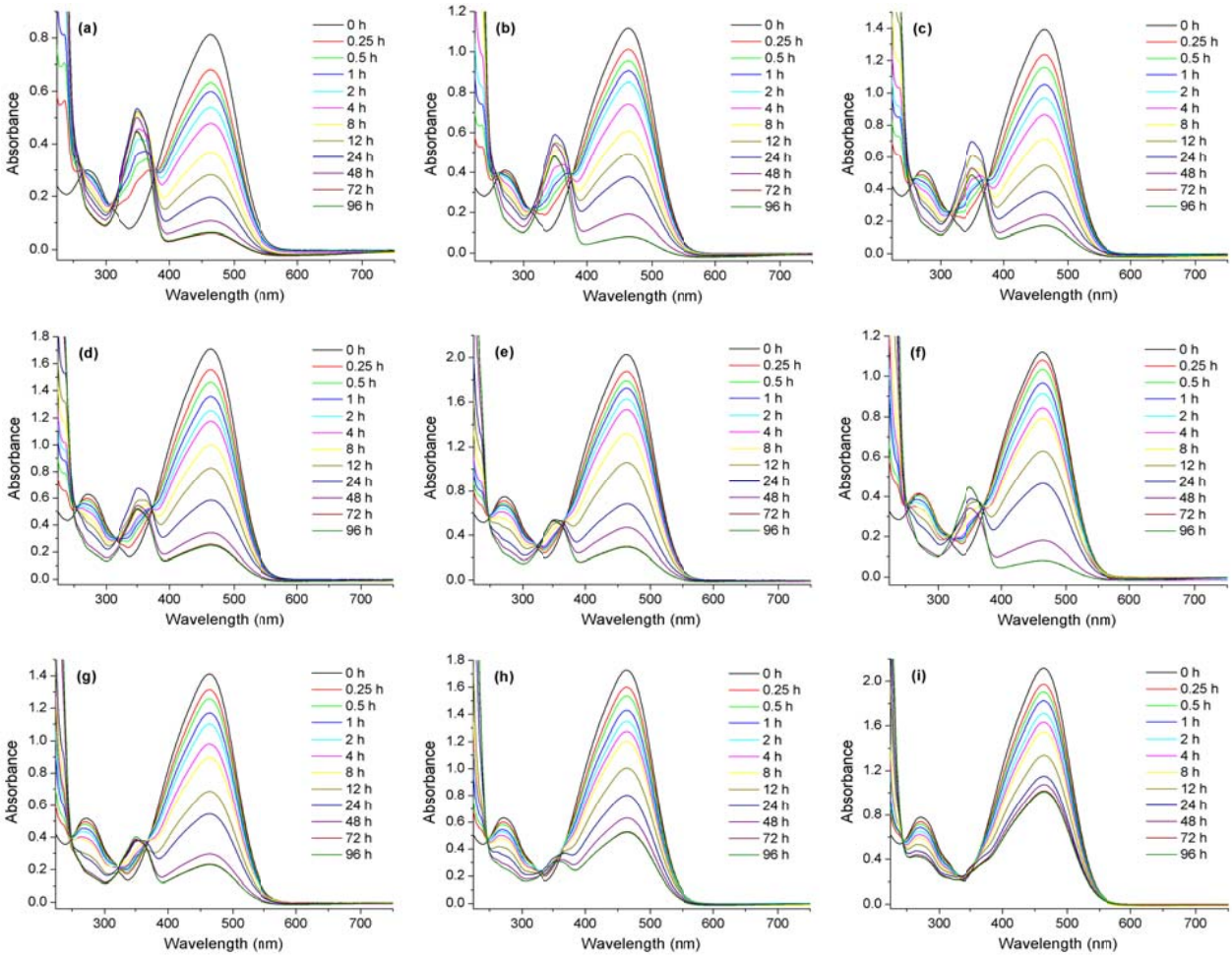

Fig. S20 UV-Vis spectra of aqueous solutions of MO during an adsorption with **1** at initial dye concentrations of (a) 10 ppm, (b) 20 ppm, (c) 30 ppm, (d) 40 ppm, (e) 50 ppm, (f) 100 ppm, (g) 150 ppm, (h) 200 ppm, and (i) 250 ppm over 0.25, 0.5, 1, 2, 4, 8, 12, 24, 48, 72, and 96 h in daylight at room temperature.

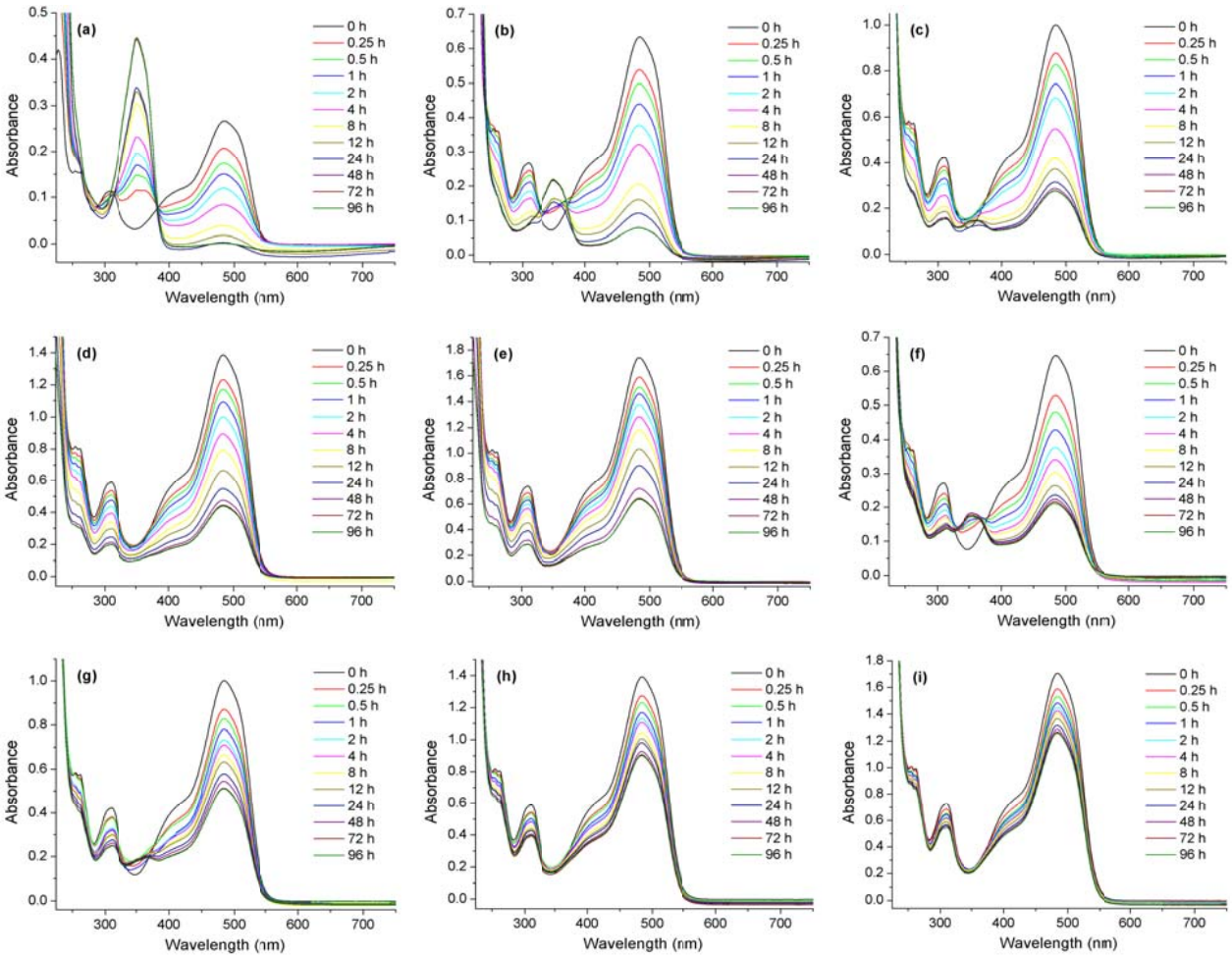

Fig. S21 UV-Vis spectra of aqueous solutions of AO7 during an adsorption with **1** at initial dye concentrations of (a) 10 ppm, (b) 20 ppm, (c) 30 ppm, (d) 40 ppm, (e) 50 ppm, (f) 100 ppm, (g) 150 ppm, (h) 200 ppm, and (i) 250 ppm over 0.25, 0.5, 1, 2, 4, 8, 12, 24, 48, 72, and 96 h in daylight at room temperature.

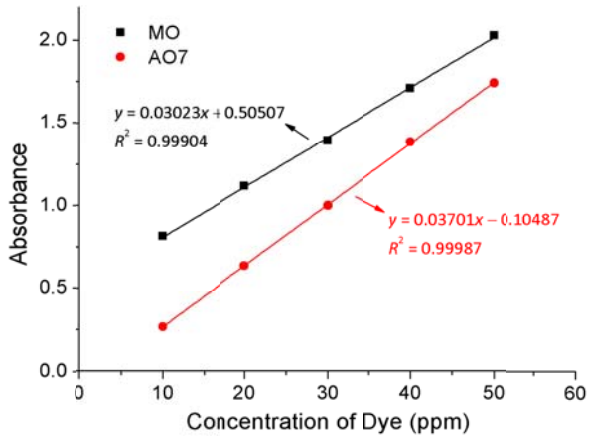

Fig. S22 Calibration curves of MO and AO7 in water in daylight at room temperature.

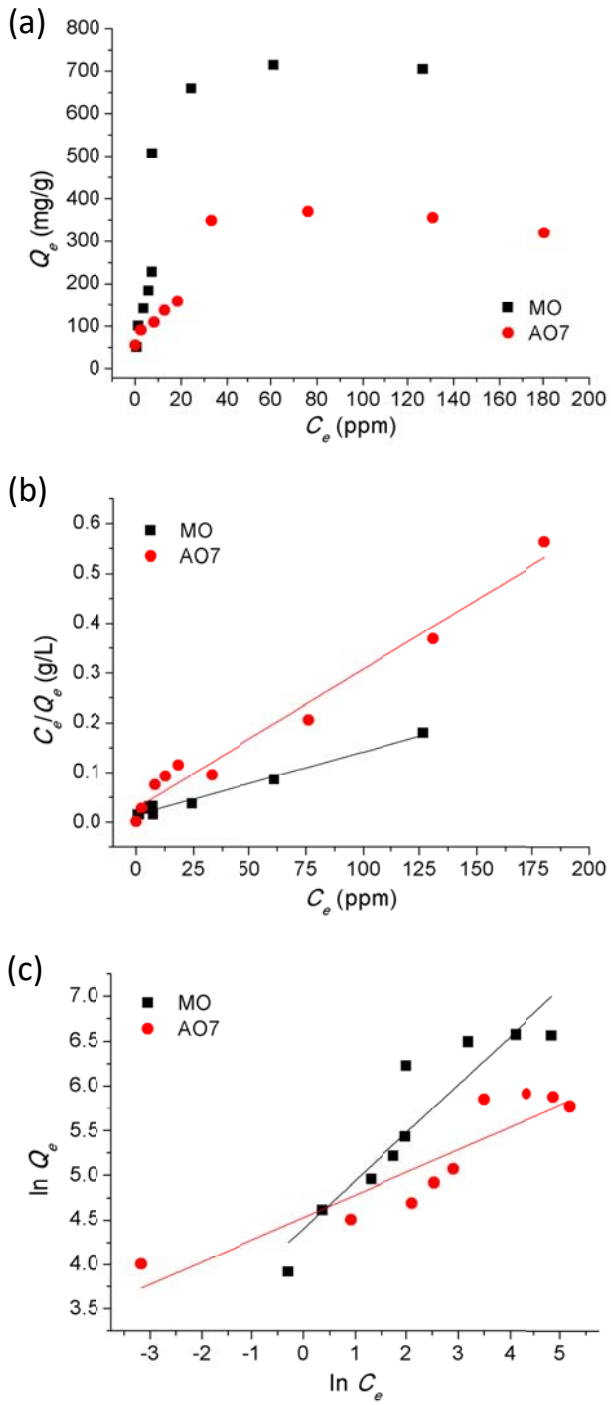

Fig. S23 (a) Adsorption isotherms for MO and AO7 over **1** in daylight at room temperature. (b) Langmuir and (c) Freundlich linear fits of MO and AO7 adsorbed onto **1**.

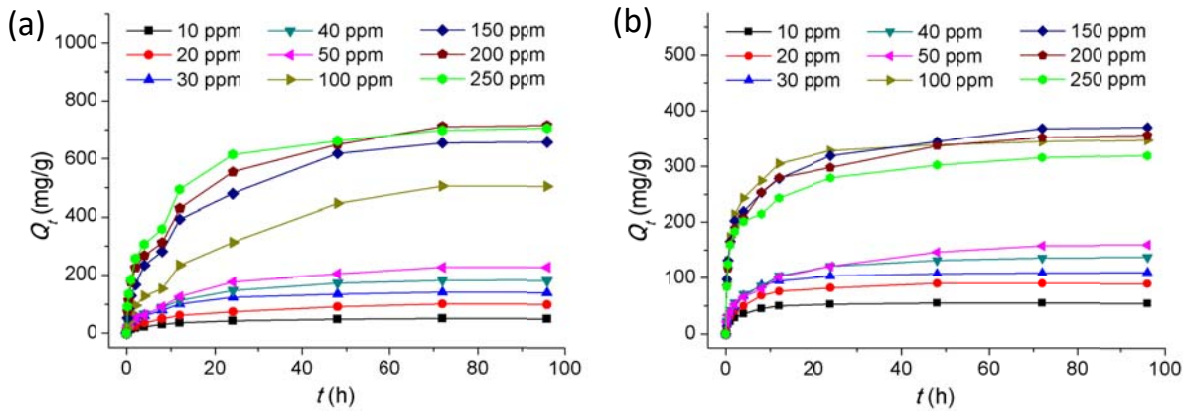

Fig. S24 Effect of contact time on the adsorption of (a) MO and (b) AO7 over **1** at different initial dye concentrations in daylight at room temperature.

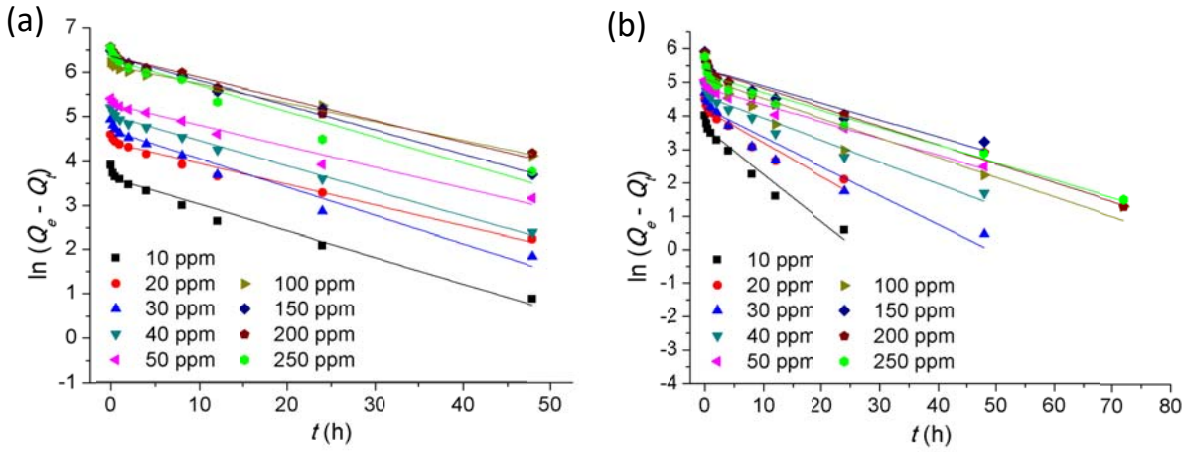

Fig. S25 Plots of pseudo-first-order kinetics for the adsorption of (a) MO and (b) AO7 over **1** in daylight at room temperature within 48 h.

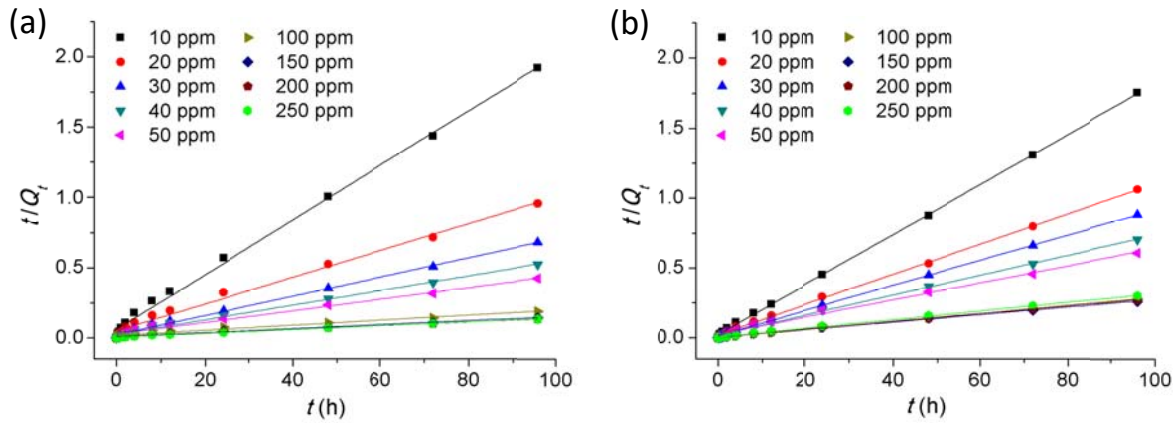

Fig. S26 Plots of pseudo-second-order kinetics for the adsorption of (a) MO and (b) AO7 over **1** in daylight at room temperature.

Table S3 Pseudo-first-order and pseudo-second-order kinetic constants for the adsorption of MO and AO7 over **1** in daylight at room temperature[a]

				Pseudo-first-order kinetic model			Pseudo-second-order kinetic model		
Dye	Condition	C_i (ppm)	$Q_{e,exp}$ (mg g^{-1})	$Q_{e,calcd}$ (mg g^{-1})	k_1 (h^{-1})	R^2	$Q_{e,calcd}$ (mg g^{-1})	k_2 (g mg^{-1} h^{-1})	R^2
MO	Daylight	10	50	37	6.02×10^{-2}	0.9674	51	5.89×10^{-3}	0.9965
		20	100	83	4.73×10^{-2}	0.9744	105	1.72×10^{-3}	0.9902
		30	141	110	6.42×10^{-2}	0.9643	146	1.90×10^{-3}	0.9964
		40	183	154	5.69×10^{-2}	0.9891	191	1.06×10^{-3}	0.9920
		50	227	199	4.75×10^{-2}	0.9762	241	5.94×10^{-4}	0.9841
		100	506	474	4.21×10^{-2}	0.9902	555	1.70×10^{-4}	0.9649
		150	658	582	5.54×10^{-2}	0.9878	694	2.38×10^{-4}	0.9882
		200	714	585	4.83×10^{-2}	0.9738	746	2.57×10^{-4}	0.9892
		250	704	540	5.82×10^{-2}	0.9416	724	3.70×10^{-4}	0.9953
AO7	Daylight	10	55	38	1.40×10^{-1}	0.9474	55	1.36×10^{-2}	0.9996
		20	90	66	9.92×10^{-2}	0.9046	92	5.32×10^{-3}	0.9991
		30	108	69	8.70×10^{-2}	0.9230	111	5.11×10^{-3}	0.9995
		40	136	97	6.52×10^{-2}	0.9508	140	2.59×10^{-3}	0.9980
		50	158	125	5.00×10^{-2}	0.9733	164	1.39×10^{-3}	0.9921
		100	348	164	5.86×10^{-2}	0.8881	350	2.29×10^{-3}	0.9996
		150	369	219	5.03×10^{-2}	0.8775	374	1.24×10^{-3}	0.9975
		200	355	217	5.61×10^{-2}	0.9604	359	1.32×10^{-3}	0.9978
		250	320	183	5.20×10^{-2}	0.9542	322	1.56×10^{-3}	0.9979

[a] C_i, initial dye concentration; $Q_{e,exp}$, experimental adsorption capacity; $Q_{e,calcd}$, calculated adsorption capacity; k_1, pseudo-first-order kinetic constant; k_2, pseudo-second-order kinetic constant.

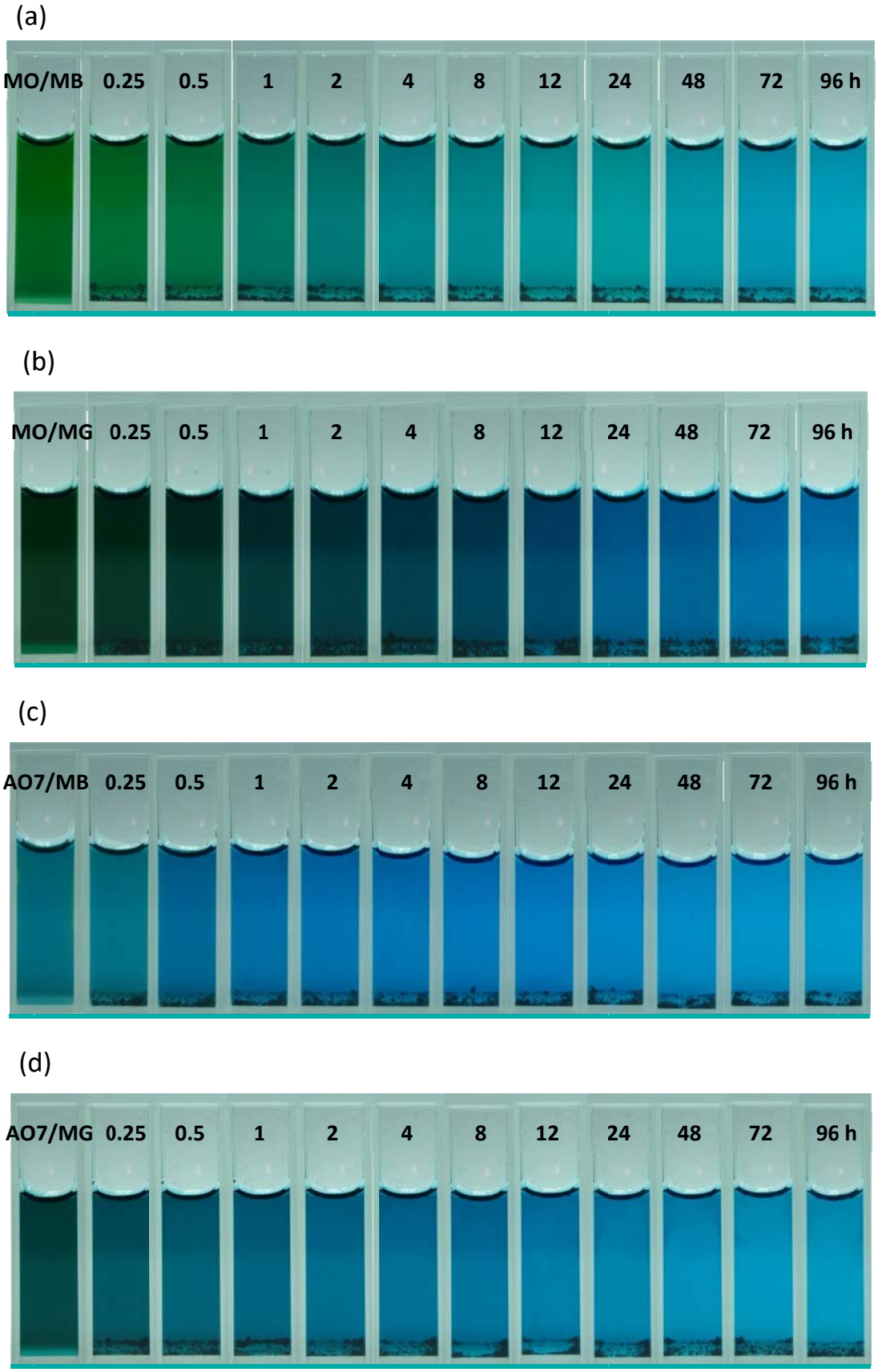

Fig. S27 Photographs of (a) MO/MB, (b) MO/MG, (c) AO7/MB, and (d) AO7/MG mixed dye solutions in water before and after adding non-activated crystalline materials of **1**, showing selective adsorption to anionic MO and AO7 dyes over cationic MB and MG dyes.

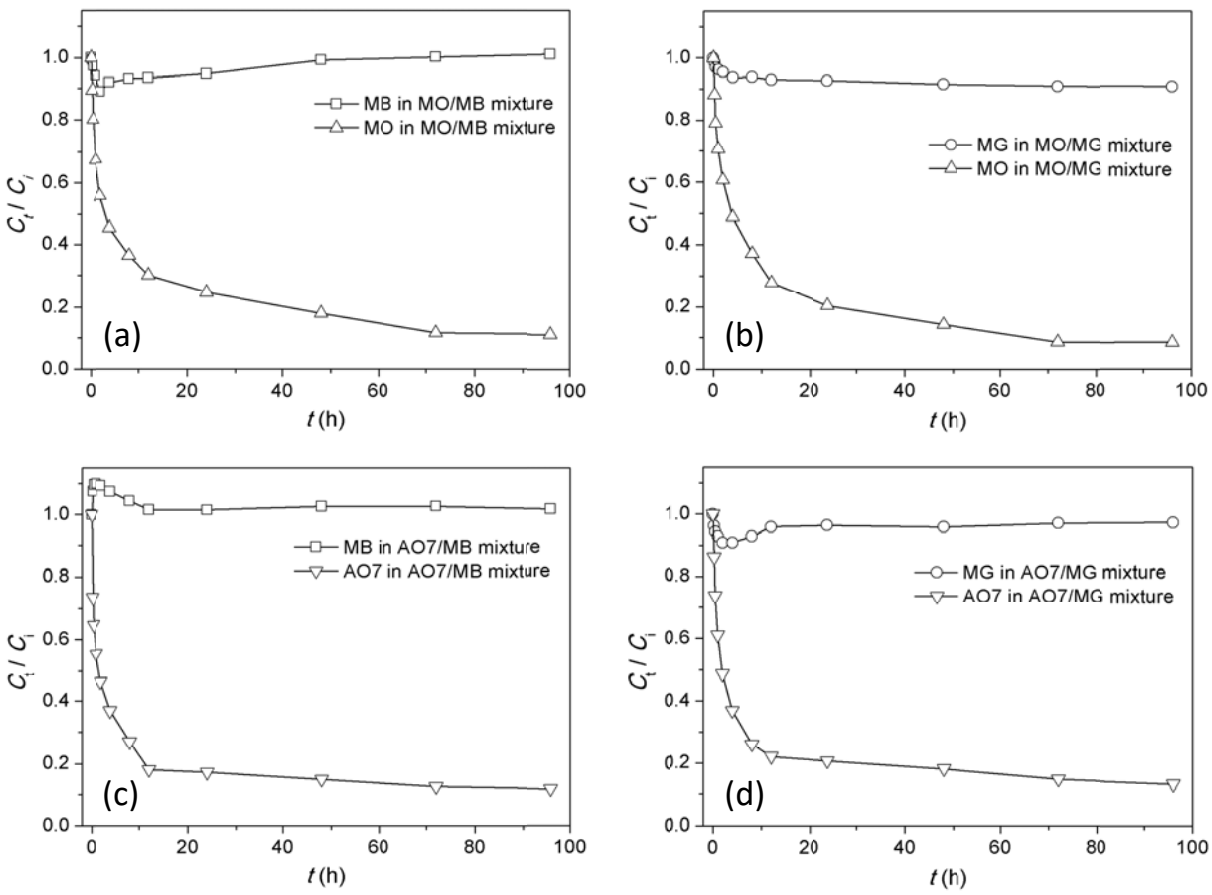

Fig. S28 Dye removal for (a) MO/MB, (b) MO/MG, (c) AO7/MB, and (d) AO7/MG mixture as a function of time over **1** in darkness at room temperature.